Fragment mass distributions in the fission of heavy nuclei by intermediate- and high-energy probes

2011 J. Phys. G: Nucl. Part. Phys. 38 085104

(http://iopscience.iop.org/0954-3899/38/8/085104)

J. Phys. G: Nucl. Part. Phys. **38** (2011) 085104 (12pp) doi:10.1088/0954-3899/38/8/085104

Fragment mass distributions in the fission of heavy nuclei by intermediate- and high-energy probes

E Andrade-II[1], J C M Menezes[2], S B Duarte[3], F Garcia[2], P C R Rossi[4], O A P Tavares[3] and A Deppman[1]

[1] Instituto de Fisica, Universidade de Sao Paulo-IFUSP, Rua do Matao, Travessa R 187, 05508-900 Sao Paulo, SP, Brazil
[2] Departamento de Ciencias Exatas e Tecnologicas, Universidade Estadual de Santa Cruz-UESC, Rodovia Ilheus-Itabuna km16, 45650-000 Ilheus-Ba, Brazil
[3] Centro Brasileiro de Pesquisas Fisicas-CBPF/MCT, Rua Dr Xavier Sigaud, 150, 22290-180, Rio de Janeiro, RJ, Brazil
[4] Divisao de Reatores, Instituto de Pesquisas Energeticas e Nucleares-IPEN/CNEN-SP, Rua do Matao, Travessa R 400, 05508-900 São Paulo, SP, Brazil

E-mail: deppman@if.usp.br

Received 25 October 2010
Published 24 June 2011
Online at stacks.iop.org/JPhysG/38/085104

Abstract

Recent experiments have shown that the multimode approach for describing the fission process is compatible with the observed results. A systematic analysis of the parameters obtained by fitting the fission-fragment mass distribution to the spontaneous and low-energy data has shown that the values for those parameters present a smooth dependence upon the nuclear mass number. In this work, a new methodology is introduced for studying fragment mass distributions through the multimode approach. It is shown that for fission induced by energetic probes ($E > 30$ MeV) the mass distribution of the fissioning nuclei produced during the intranuclear cascade and evaporation processes must be considered in order to have a realistic description of the fission process. The method is applied to study ^{208}Pb, ^{238}U, ^{239}Np and ^{241}Am fission induced by protons or photons.

1. Introduction

There is a growing interest on the fission process and on its products due to its importance in applications such as nuclear reactors and nuclear medicine. The possibility of transmutation of nuclear waste [1–3] from traditional reactor in the so-called brewing reactors, for instance, has attracted the attention of researchers willing to solve the long-standing problem of storage of the radioactive material produced in nuclear reactors. The mass distributions of fission fragments are fundamental information to development brewing reactors as well as to understand material damage induced by radiation from nuclear fuel.

Fission-fragment mass distributions can also give much information about the fission mechanism, allowing the study of the dynamical process leading to nuclear fission [4, 5]. The different processes by which fission takes place can result in different masses of the fragments produced. Theoretically, the fission process has been successfully described by the statistical scission model (SSM) [6–8], which takes into account the collective effects of nuclear deformation during fission through a liquid-drop model, and includes single-particle effects through microscopic shell-model corrections. The microscopic corrections create valleys in the space of elongation and mass number, each valley corresponding to one different fission mode [8]. The fission cross section results from the incoherent sum of the contributions of each channel, $\sigma_i(A, Z)$, which are usually written in the form

$$\sigma_i(A, Z) = \frac{K_i}{\sqrt{2\pi}\Gamma_i} \exp\left[-\frac{(A - A_i)^2}{2\Gamma_i^2}\right] \sigma(Z), \tag{1}$$

where K_i is the intensity of the ith channel, the parameter A_i is the position of the most probable mass for the fission fragments and Γ_i is the width of the mass distribution according to SSM.

For the charge distribution, $\sigma(Z)$, many authors utilize the approach of a uniform-charge distribution (UCD), where it is assumed that the charge density of the fragments is the same as that for the fissioning nucleus. However, it has been shown [9] that for actinides the fragment charge distribution is better described by a Gaussian function

$$\sigma(Z) = \frac{1}{\sqrt{2\pi}\Gamma_Z} \exp\left[-\frac{(Z - \overline{Z_0})^2}{2\Gamma_Z^2}\right], \tag{2}$$

where Γ_Z is the width of the charge distribution and $\overline{Z_0}$ is the most probable charge.

Combining this Gaussian distribution for the atomic number with the mass number distributions according to the multimode model one gets the yield of fragments produced in intermediate- and high-energy fissions of actinides [10, 11]:

$$\sigma(A, Z) = \left\{ \sum_i \left[\frac{K_i^{\mathrm{L}}}{\sqrt{2\pi}\Gamma_i^{\mathrm{L}}} \exp\left(-\frac{\left(A - A_i^{\mathrm{L}}\right)^2}{2\left(\Gamma_i^{\mathrm{L}}\right)^2}\right) + \frac{K_i^{\mathrm{H}}}{\sqrt{2\pi}\Gamma_i^{\mathrm{H}}} \exp\left(-\frac{\left(A - A_i^{\mathrm{H}}\right)^2}{2\left(\Gamma_i^{\mathrm{H}}\right)^2}\right) \right] + \frac{K_{\mathrm{S}}}{\sqrt{2\pi}\Gamma_{\mathrm{S}}} \exp\left(-\frac{(A - A_{\mathrm{S}})^2}{2(\Gamma_{\mathrm{S}})^2}\right) \right\} \frac{1}{\sqrt{2\pi}\Gamma_Z} \exp\left(-\frac{(Z - \overline{Z_0})^2}{2\Gamma_Z^2}\right), \tag{3}$$

where the summation runs over the asymmetric modes. The parameters for the symmetric mode are K_{S}, A_{S} and Γ_{S}, while $K_i^{\mathrm{H(L)}}$, $A_i^{\mathrm{H(L)}}$ and $\Gamma_i^{\mathrm{H(L)}}$ are the parameters for the heavy (light) fragment produced in the asymmetric mode i. For the atomic number distribution the parametrization used is [9]

$$\overline{Z_0} = \mu_1 + \mu_2 A \tag{4}$$

for the most probable atomic number of the fragment, and

$$\Gamma_Z = \nu_1 + \nu_2 A \tag{5}$$

for the width of the atomic number distribution. μ_1, μ_2, ν_1 and ν_2 are the fitting parameters. The dependence of distributions on the atomic number will not be relevant in the following discussion.

Yield, position and width parameters for each mode in equation (3) and μ_1, μ_2, ν_1 and ν_2 in (4) and (5) are usually considered free parameters for the fitting procedure. This method has been used for describing spontaneous fission [12], low-energy induced fission [13–15], fission induced by thermal neutrons [16–18] and 12 MeV protons [19], and even for fission induced by intermediate-energy probes such as 190 MeV protons [20], neutrons at energies

up to 200 MeV [21], and also by heavy-ions [22, 23]. More recently, it has been applied for describing ^{238}U fission induced by photons from bremsstrahlung [10] with end-point energies of 50 and 3500 MeV, and fission induced by 660 MeV protons on ^{241}Am and ^{237}Np [11]. The results obtained have shown that for most of the actinide nuclei three modes are needed for explaining the existing experimental data, namely the symmetric (superlong, SL) mode, and two asymmetric modes, the standard I (S1) and the standard II (S2). For some nuclei, however, additional modes have to be included [4]. In many works, the parameters for the asymmetric modes for heavy and light fragments are not considered independent, usually being related through the equations $\Gamma_i^{\mathrm{L}} = \Gamma_i^{\mathrm{H}}$, $K_i^{\mathrm{L}} = K_i^{\mathrm{H}}$ and $A_i^{\mathrm{L}} = 2A_{\mathrm{S}} - A_i^{\mathrm{H}}$.

With the advent of new experimental facilities, such as the Fragment Separator (FRS) at GSI, the fission-fragment mass distributions can be measured with great accuracy, and fragments coming from different processes, such as spallation or fragmentation, can be separated experimentally. A systematic study of the values obtained for the parameters in formula (3) by fitting to experimental data for spontaneous or low-energy fission of several nuclei was performed by Böckstiegel *et al* [15], showing that those parameters can be described by smooth functions of the fissioning nucleus mass number. In this work, a new method for the analysis of fragment mass distributions from fission induced by intermediate- and high-energy probes is developed. The main feature of this method is that it takes into account the fissioning nucleus distributions that are generated in intermediate- or high-energy nuclear reactions.

The paper is organized as follows: section 2 shows a discussion of the effects of the fissioning system distributions on the fragment mass distributions calculated in the multimodal approach; section 3 describes a Monte Carlo method used for obtaining fissioning system distributions, where intranuclear cascade and evaporation processes are considered; section 4 describes two different calculations where the new methodology is applied with two sets of parameters for the multimodal calculations; in section 5 the method is used to describe the mass distribution of fission fragments produced in the fission of ^{208}Pb induced by 500 MeV and in section 6 the conclusions are presented.

2. The problem of the fissioning nucleus

Whereas, for spontaneous or low-energy fission the parameter A_{S} in (3) may be correctly substituted by $A_{\mathrm{o}}/2$, with A_{o} being the mass number of the target nucleus, for the fission induced by intermediate- or high-energy probes this substitution cannot be done, and A_{S} is then a free parameter in the fitting procedure, which is associated with the mass number of the fissioning nucleus, A_{f}. This mass number, however, depends on the probe used, its incident energy and the properties of the target nucleus. Moreover, it is rather a mass distribution (see figure 1), not a fixed value. The parameter A_{S} must be, indeed, interpreted as the mean value for the mass of the symmetric fission fragment.

At intermediate and high energies, the values for the position and width for each fission mode, as obtained by direct fitting of the expression of the type shown by equation (3), may be altered because of the fissioning nuclei mass and atomic number distributions [24, 25]. The effects of the A_{f}-distribution on the parameters describing the multimode fission have already been observed in 1 GeV/nucleon ^{238}U on deuterium reaction [24], and may also have effects on the results obtained by intermediate-energy photon and proton reactions [10, 11]. Therefore, at intermediate and high energies, the fragment mass distributions are folded into the fissioning system mass distributions. A more realistic calculation of fission-fragment mass distribution must take into account the broad mass distributions of the fissioning nuclei. As it will be shown in the following, these distributions not only affect the calculated fragment mass distributions, but also are dependent on the probe used and on its incident energy.

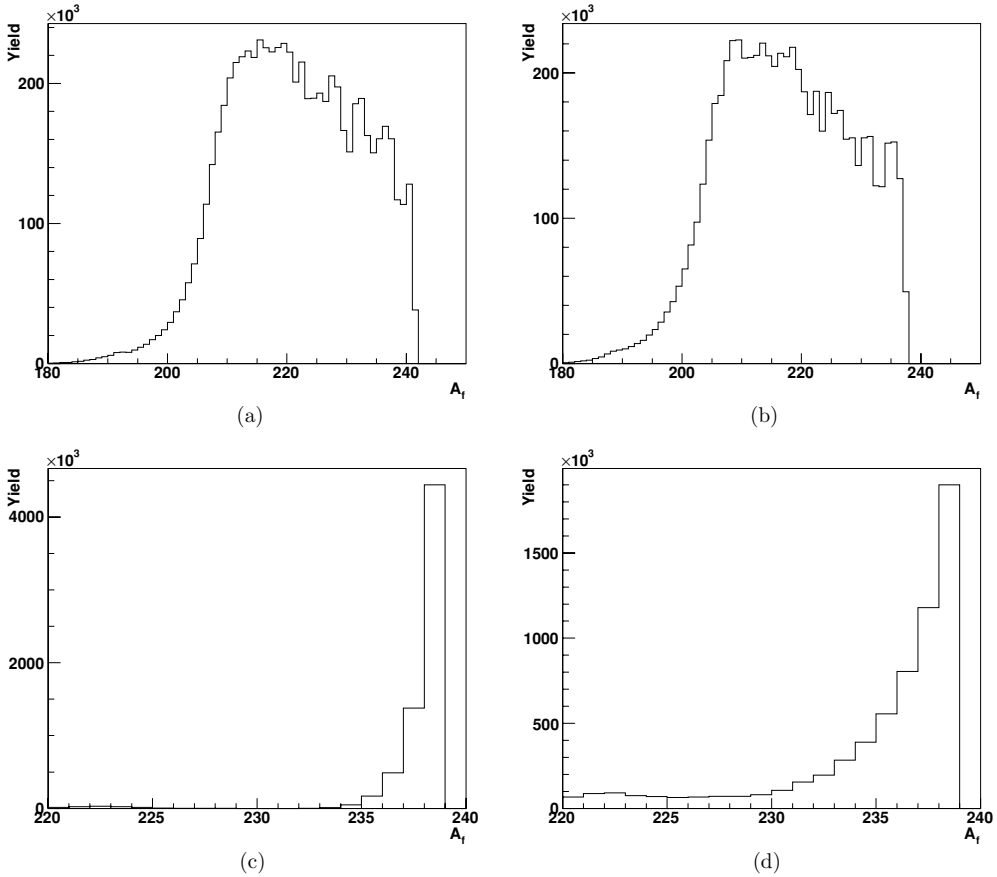

Figure 1. Mass distribution of the fissioning nucleus in reactions induced by 660 MeV protons on ^{241}Am (a) and ^{237}Np (b) target nuclei and in the fission of ^{238}U induced by bremsstrahlung with end-point energies of 50 MeV (c) and 3500 MeV (d) as obtained by the CRISP code.

It is possible to unfold the contributions due to fission modes and to fissioning nuclei distribution in the fragment mass distribution by using Monte Carlo methods and to obtain values for the multimode parameters corresponding to each fission mode by taking into account the A_f-distributions. CRISP is a Monte Carlo code for simulating nuclear reactions [26] that uses a two-step process. First, an intranuclear cascade is simulated following a time-ordered sequence of collisions in a many-body system [27, 28], and when the intranuclear cascade is finished the evaporation of nucleons and alpha particles starts in competition with fission [29].

In the simulation, reactions can be initiated by intermediate- and high-energy protons [28] or photons [30–32]. It has been extended to energies up to 3.5 GeV [33], and it was shown that the CRISP code can give good results for total photonuclear absorption cross sections from approximately 50 MeV, where the quasi-deuteron absorption mechanism is dominant, up to 3.5 GeV, where the so-called photon-hadronization mechanism is dominant, leading to a shadowing effect in the cross section [33]. One important feature in the simulation of the intranuclear cascade is the Pauli blocking mechanism, which avoids violation of the Pauli principle. In CRISP, a strict verification of this principle is performed at each step of the cascade, resulting in a more realistic simulation of the process. The advantages of such an approach have been discussed elsewhere (see [26] and references therein).

Table 1. Values for some of the relevant parameters in the multimode formula for the fission-fragment mass distributions. The low-energy parameters are those obtained from the systematic study for spontaneous and low-energy fission [15] (here the errors are estimated range), those for ^{241}Am and ^{237}Np are results of fittings for 660 MeV protons [11], and the parameters for uranium are those obtained from fittings to data of fission induced by bremsstrahlung photons with end-point energies of 50 and 3500 MeV [10].

Parameter	Low energy	^{241}Am	^{237}Np	^{238}U (50 MeV)	^{238}U (3500 MeV)
Γ_S	10.0 ± 2	15.0 ± 0.9	13.7 ± 1.0	12.0 ± 0.48	12.0 ± 0.48
A_1^H	135.0 ± 1	133.5 ± 0.72	133.0 ± 0.98	133.32 ± 1.03	133.32 ± 1.03
Γ_1^H	3.75 ± 2	4.2 ± 0.5	4.5 ± 0.4	3.54 ± 0.4	3.54 ± 0.4
A_2^H	141.0 ± 2	139.0 ± 1.17	138.0 ± 1.03	137.5 ± 1.41	137.5 ± 1.41
Γ_2^H	5.0 ± 1	7.0 ± 0.5	6.5 ± 0.6	6.0 ± 0.21	6.0 ± 0.21
		Type 1	Calculation		
$K_S(mb)$	–	2970.0 ± 20.5	2590.0 ± 23.3	23.75 ± 0.7	23.75 ± 0.7
$K_1(mb)$	–	45.8 ± 0.2	49.0 ± 0.3	7.5 ± 0.04	7.5 ± 0.04
$K_2(mb)$	–	220.5 ± 1.5	252.0 ± 1.3	140.0 ± 7.2	140.0 ± 7.2

In the evaporation/fission competition that follows intranuclear cascade, Weisskopf's model is adopted for calculating the branching ratios of the evaporating channels, which includes evaporation of neutrons, protons and alpha particles [29, 31, 32] and the Bohr–Wheeler model is adopted for fission. The code has provided photofission cross sections in good agreement with experimental data [26]. The CRISP code has already been used for evaluating mass distributions of fragments for fission induced by photons at intermediate energies [25], and to calculate spallation yields and neutron multiplicities for reactions induced by high-energy protons [34], giving results in good agreement with experimental data. Also, the code has already been used in the studies of the ADS (accelerator driving system) nuclear reactors [34–37].

This work reports on a study of the characteristics of the different fission modes, as observed through the fission-fragment mass distributions, applying the multimode fission approach to individual fissioning nuclei. Effects of fissioning nucleus mass number and atomic number distributions are included in the Monte Carlo simulations with the CRISP code, and the widths and peak positions for each fission mode are those obtained from the systematic analysis of low-energy fission (first column in the upper table 1). Thus, no free parameters are used here, the results being dependent only on the fissioning system formed at the end of the reaction simulated through the intranuclear cascade and evaporation/fission competition, and on the parameters of the multimode description of the fission process. It is considered the possibility for fission through the three most important modes, namely superlong, standard I and standard II.

3. Monte Carlo simulations with the CRISP code

As mentioned before, CRISP simulation is performed in a two-step framework: intranuclear cascade and evaporation/fission competition. To simulate intermediate- and high-energy reactions, due to computational reasons, it is usually better to simulate a number N_c of cascades, recording all relevant information about the residual nuclei, which are kept in a file as triplets containing mass number, A_R, atomic number, Z_R, and excitation energy, E_R, formed

at the end of the intranuclear cascade. Afterward, the values A_R, Z_R and E_R in the triplets are used as input to perform the evaporation/fission competition process. A number N_{ef} of simulations are performed for each residual nucleus obtained at the end of the intranuclear cascade, so that at the completion of the simulation one has a total of $N_t = N_c\, N_{ef}$ simulated events for the evaporation/fission process.

The present analysis focuses on the results obtained with 660 MeV protons on ^{241}Am and ^{237}Np target nuclei, and on bremsstrahlung with end-point energies of 50 MeV and 3500 MeV on ^{238}U. The number of intranuclear cascade events was $N_c = 3000$, and the number of evaporation/fission simulations for each residual nucleus was $N_{ef} = 2500$, so that the total number of simulated processes was $N_t = 7.5 \times 10^6$ events. For bremsstrahlung photons on ^{238}U the energy, ω, was sorted according to a distribution $B(\omega) = C/\omega$ (C is a normalization constant). Although all nuclei studied show high fissility values, not all simulated events end at the fission process, and some of them generate spallation products.

Whenever the fission channel is chosen, the masses and atomic numbers of the heavy fragments produced, A^H and Z^H, respectively, are sorted according to a probability distribution given by

$$p(A, Z) = \left\{ \sum_i \frac{p_i}{\sqrt{2\pi}\Gamma_i} \exp\left[-\frac{(A - A_i)^2}{2\Gamma_i^2} \right] \right\} \frac{1}{\sqrt{2\pi}\Gamma_Z} \exp\left[-\frac{(Z - \overline{Z_0})^2}{2\Gamma_Z^2} \right], \tag{6}$$

where p_i is the probability that fission occurs through the ith mode which is related to the intensities K_i by the relation

$$p_i = \frac{K_i}{\sum_i K_i}, \tag{7}$$

the index $i = S, 1, 2$ corresponding to the modes SL, $S1$ and $S2$, respectively. The light fragments are obtained according to $A^L = A_f - A^H$ and $Z^L = \overline{Z_0} - Z^H$. The Z dependence of the probability is explicitly shown in (6) for the sake of completeness only, since it will not be relevant in the results presented in this work.

It is important to stress that the evaporation process has as input the distribution of nuclei obtained at the end of the intranuclear cascade; therefore, the fissioning nucleus may be different from the cascade residual nucleus because some neutrons, protons and/or alpha-particles are allowed to evaporate before fission takes place. The mass distributions of the fissioning nucleus are shown in figure 1. For both target nuclei, the distributions are wide and asymmetric, and of course the related distributions for A_S, which is a relevant parameter in equation (6), show the same shape. In many works, these distributions are not considered, and A_S is used as a free parameter. This kind of substitution has effects on the values obtained for the other free parameters used for fitting formula (3) to experimental data, such as the peak position and width of the Gaussian distributions representing each channel, as discussed above.

In the systematic study carried out by Böckstiegel *et al* [15], for spontaneous fission and low-energy reactions, the fissioning nuclei can be considered identical to the initial (or target) nuclei, and thus the problem due to fissioning nuclei properties does not arise. On the other hand, fittings to fission data obtained for high energies lead to values of the parameters that deviate from the systematics at low-energy fission. Based on this systematics for low-energy or spontaneous fission, one obtains the estimated values for the relevant parameters in (6), which are shown in table 1 (upper part), and compares them to the corresponding values obtained by fittings of high-energy fission data. One can see that for high-energy reactions the width obtained for the symmetric channel is systematically higher than those obtained with low energy or spontaneous fission data, and the position for the peak in the asymmetric fission

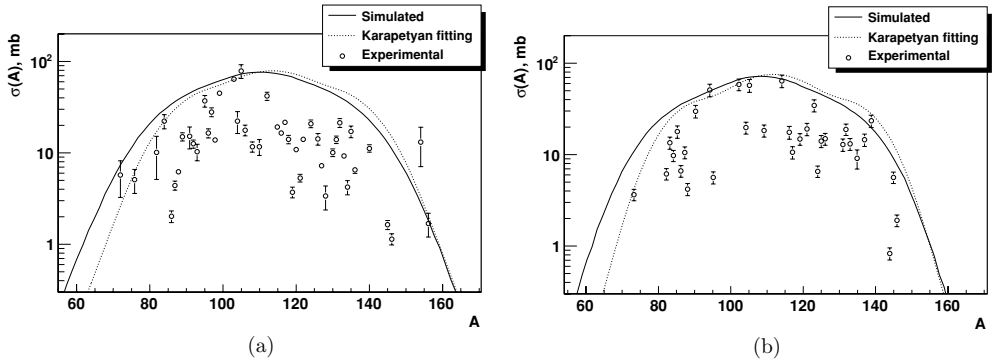

Figure 2. Fragment mass distribution for fission induced by 660 MeV protons on ^{241}Am (a) and ^{237}Np (b) targets using values from Karapetyan *et al* [11] (· · · · · ·) for the parameters corresponding to the three fission modes considered in this work and as calculated with the CRISP code (——) by using the fissioning nucleus mass distribution and keeping all other parameters in the mass distribution formula equal to those found by Karapetyan *et al.* The open symbols (◯) represent the experimental data [11].

masses is shifted down with respect to the systematic values. This is an evidence of the effect of fissioning system distributions on the values obtained in the multimode analysis.

Using the CRISP code it is possible to separate the effects of the fission-channel width and those of the mass distribution of the fissioning nucleus because the fission process is considered for each individual fissioning nucleus. Note that in expression (6) the symmetric fragment mass, A_S, is no more a free parameter, but it is completely determined by simulations with the CRISP code till the fission point. The effects of using the fissioning system distribution instead of the free parameter A_S can be observed in figure 2, where the two methods are compared. Here, the results obtained by Karapetyan *et al* [11] are plotted along with the simulation with the CRISP code, where the values for yields, peak positions and widths used are the same as those used in [11].

It is possible to observe that the simulated results are shifted to lower masses with respect to the calculated ones. Besides, the simulated width is somewhat larger due to the mass distribution of the fissioning nucleus, and some structures observed in the calculated curve, due to the different mode contributions, are smoothed in the simulation results, again due to the initial distribution of mass numbers. This result corroborates the conclusion obtained in [24] about the effects of the distribution of fissioning systems on the analysis of the fission channel when intermediate- and high-energy probes are used to induce fission in the target nucleus.

Note that the mass dependence on the multimode parameters is not considered here, and that the shift observed is due to the fact that the distributions presented in figure 1 are not symmetric. The effects of the fissioning nuclei distributions will be more relevant when the dependence of the multimode parameters on the mass of the fissioning nucleus is included, as shown below.

4. Multimode parameters

In the following, the methodology outlined above is used to study the fission process at high excitation energies. It is interesting to investigate fission induced by photons and by protons, since these probes lead to the formation of different fissioning systems. In fact, comparing the

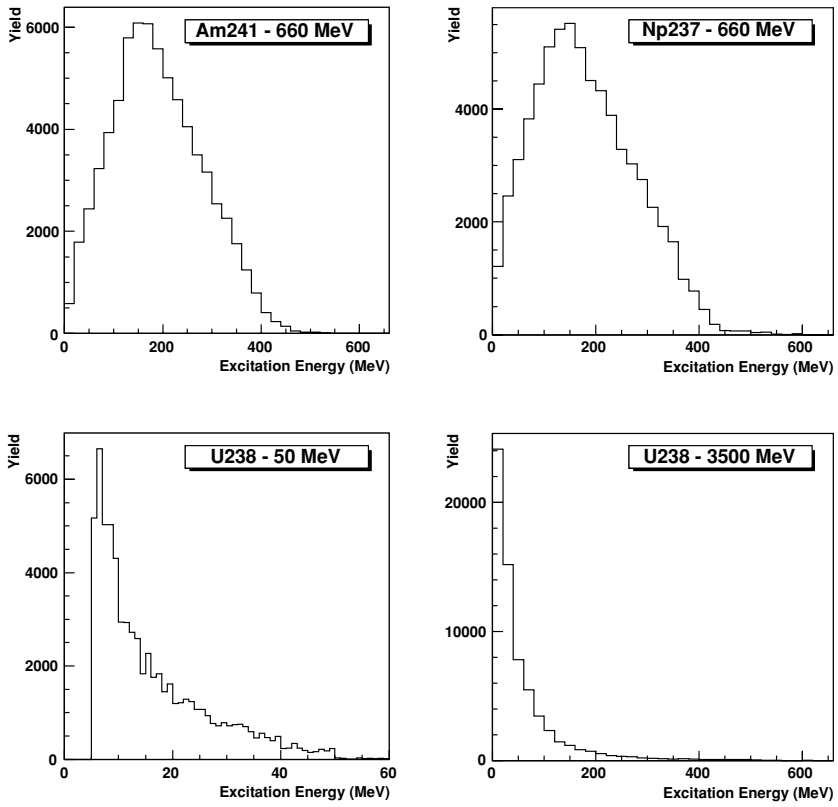

Figure 3. Excitation energy distributions of the fissioning nuclei obtained with the CRISP code for different fission reactions of heavy nuclei as indicated.

mass distribution of the fissioning nuclei for reactions induced by photons from bremsstrahlung with end-point energies of 50 MeV and 3500 MeV shown in figures 1(c) and (d) with those for reactions induced by 660 MeV protons shown in figure 1 it is possible to observe that the A_f distributions obtained with these probes are very different.

For the determination of the fission fragment masses it will be necessary to attribute values for the parameters used in the multimode approach, which is not a trivial problem. As observed in figure 1, the mass number of fissioning nuclei varies over a broad range, and the multimode parameters that appear in equation (6) are not determined for all of them. Also, as shown in figure 3, the excitation energies of the fissioning nuclei are in many cases around hundreds of MeV, and the parameters are not determined at these energies.

It was believed that at low energies fission should be predominantly asymmetric, while at high energies the symmetric mode should be dominant because at these energies the effects due to nuclear structure would be washed out. However, Siegler *et al* [38] showed that there is an important contribution of the symmetric mode even at energies around 5 MeV. Therefore, the calculation has to include contributions from the symmetric and asymmetric modes with corresponding intensities depending on the fissioning nucleus mass. In this work, two different calculations were carried out. One calculation (type 1) was performed by using for K_S, K_1 and K_2 the values found by Demekhina *et al* and Karapetyan *et al* [10, 11], which are presented in table 1 (lower part) to calculate the corresponding probabilities through equation (7), while

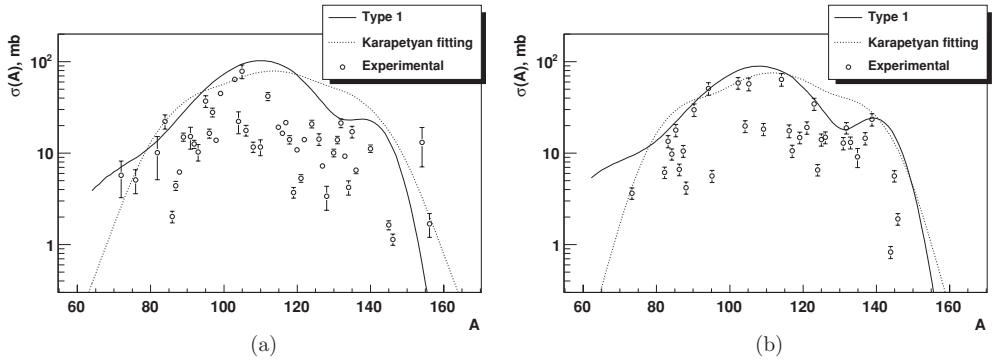

Figure 4. Fragment mass distribution for fission induced by 660 MeV protons on ^{241}Am (a) and ^{237}Np (b) targets considering calculation type 1 (——) using the values for K_S, K_1 and K_2 presented in table 1 (lower part). Best fit found in [11] is represented by the dotted line (· · · · · ·). All results are compared with experimental data (◯) [11].

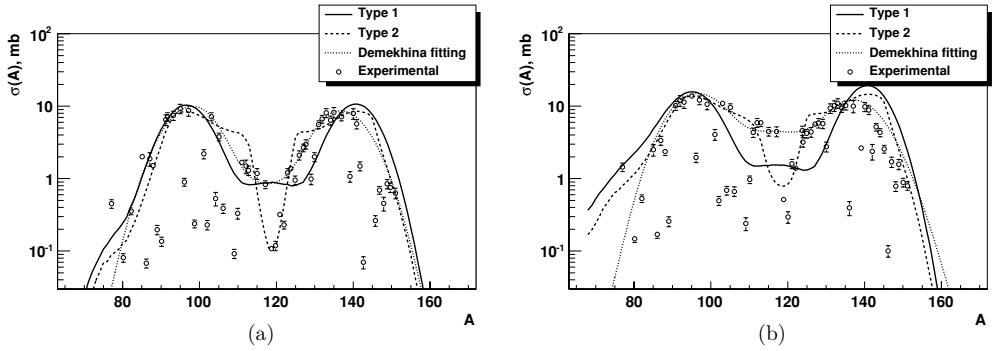

Figure 5. Fragment mass distribution for fission of ^{238}U induced by bremsstrahlung of 50 MeV (a) and 3500 MeV (b) end-point energies considering calculation type 1 (——) using the values for K_S, K_1 and K_2 presented in table 1 (lower part) and type 2 (- - - -) performed considering the probabilities $p_{(S,1,2)}$ as Gaussian functions of the fissioning nucleus mass number. The dotted line (· · · · · ·) represents the best fit of the formula (3) as done by Demekhina *et al* [10] and open circles (◯) are their experimental results.

keeping all other parameters unchanged. The second calculation (type 2) was performed considering the probabilities $p_{(S,1,2)}$ as Gaussian functions of the fissioning nucleus mass number, which are obtained by fitting the systematic values from Böckstiegel *et al* [15] and using linear extrapolation to lower masses ($A < 220$). Again all other parameters are kept unchanged.

In figures 4 and 5 the results obtained are compared to experimental data and to the fitted distributions from [10, 11]. Type 1 and type 2 calculations are quite different from the calculations performed in [10, 11]. These results show that the effects of the fissioning nucleus mass distributions are significant, and that it must be included in a realistic calculation.

The comparison with the experimental data shows that the calculations correctly describe the position and width of the fragment mass distributions. More accurate data for heavy nuclei fission induced by energetic probes would be useful for extracting information about the fission process.

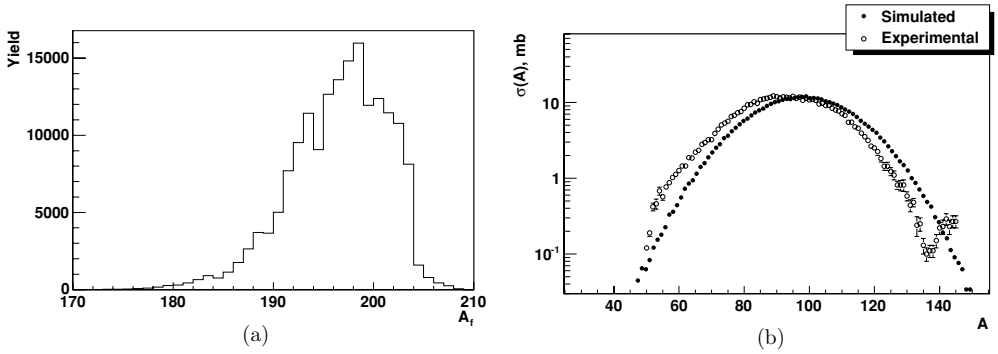

Figure 6. (a) Mass distribution of the fissioning nucleus in reactions induced by 500 MeV protons on the ^{208}Pb target nucleus as obtained by the CRISP code. (b) Fragment mass distribution for fission induced by 500 MeV protons on ^{208}Pb as simulated by CRISP (——circle). Experimental data are from GSI [39] (◯).

5. Application of the method to ^{208}Pb fission induced by 500 MeV protons

Precise measurements of fragment mass distributions were obtained for fission induced by high-energy protons at GSI [39]. Here, the newly introduced method will be used to describe the experimental results obtained for the reaction p (500 MeV) + ^{208}Pb.

The fissioning nucleus mass distribution is shown in figure 6(a), and it is possible to observe a broad mass distribution around A $\sim$ 198. This distribution shows that the method outlined above is necessary for a correct description of the fragment mass distribution.

Unfortunately, there is not any systematic study of the multimodal parameters in the mass region of interest in this case. To obtain those parameters, we used a linear extrapolation of the data from the systematics for K_S for masses below $A = 220$, and used the Gaussian fits from calculation type 2 for K_1 and K_2.

For heavy fragment distributions the peak for the asymmetric modes are calculated by

$$A_1^H = a_1 A_f + a_2 \tag{8a}$$
$$A_2^H = a_3 A_f + a_4, \tag{8b}$$

while the width for each mode is assumed to be constant, with

$$\Gamma_S = a_5 \tag{9a}$$
$$\Gamma_1^H = a_6 \tag{9b}$$
$$\Gamma_2^H = a_7. \tag{9c}$$

The linear behavior for peak position and width is in agreement with the behavior of the parameters for the low-energy fission [15]. In table 2, the best values obtained are presented, and in figure 6(b) the fission fragment mass distribution calculated according to the method developed in this work is plotted and compared with experimental data.

The results presented in figure 6(b) show a fair agreement between calculation and experiment. The calculated distribution reproduces the shape of the experimental distribution remarkably well, but there is a shift of 9.82 ± 0.05 mass units of the overall distribution toward the high mass region. This shift could be corrected by including the emission of prompt neutrons during the fission process and including the evaporation of nucleons and clusters from the fission fragments.

Table 2. Values of the relevant parameters found for the best agreement between simulated and experimental data for the fission of ^{208}Pb induced by 500 MeV protons. Errors indicated represent the superior limit for uncertainties.

Parameter	Value
a_1	0.01 ± 0.05
a_2	121.68 ± 0.05
a_3	0.23 ± 0.05
a_4	125.66 ± 0.05
a_5	14.93 ± 0.05
a_6	3.97 ± 0.05
a_7	5.21 ± 0.05

6. Conclusions

In this work, a Monte Carlo calculation method has been used for simulating the fission process in reactions of 660 MeV protons on ^{241}Am and ^{237}Np, 500 MeV protons on ^{208}Pb and for bremsstrahlung with end-point energies of 50 and 3500 MeV on ^{238}U. First, it was observed that these reactions result in fissioning nuclei of very different masses. Also it was shown that the mass distribution of the fissioning system has evident effects on calculated fragment mass distributions.

The fission fragment masses were obtained according to the multimode approach based on the statistical scission model, with three different assumptions for the relevant parameters, namely the symmetric mode dominance, fixed probabilities for each mode and probabilities dependent on the mass numbers of the fissioning nuclei. The mass dependence of the fission mode probabilities was determined by fitting Gaussian functions to the low-energy systematics for the parameters used in the multimode approach. None of the parameters was determined by fitting mass distributions.

The results show that fissioning nucleus distributions are relevant for intermediate- and high-energy induced fissions, and one needs to take them into account in the calculation of fragment mass distributions.

Applying the method introduced here to analyze the p(500 MeV) + ^{208}Pb fission data, fair agreement is obtained between calculation and experiment. The result can be improved if prompt neutron emission and/or fragment de-excitation via nuclear evaporation are included.

Acknowledgment

This work was supported by CNPq and FAPESP, Brazilian agencies.

References

[1] Biergersson E, Oberstedt S, Oberstedt A, Hambsch F-J, Rochman D, Tsekhanovich I and Raman S 2007 *Nucl. Phys.* A **791** 1–23
[2] Department of Nuclear Energy Research Advisory Committee and the Generation IV International Forum 2002 *A Technology Roadmap for Generation IV Nuclear Energy Systems* GIF-002-00
[3] Rubbia C *et al* 1995 Conceptual design of a fast neutron operated high power energy amplifier *European Organization for Nuclear Research Report* CERN/AT/95-44(ET)
[4] Pashkevich V V and Rusanov A Ya 2008 *Nucl. Phys.* A **810** 77–90
[5] Maslov V M 2007 *Phys. Lett.* B **649** 376–83
[6] Pashkevich V V 1971 *Nucl. Phys.* A **169** 275–93

[7] Wilkins B D, Steinberg E P and Chasman R R 1976 *Phys. Rev.* C **14** 1832–63
[8] Brosa U, Grossmann S and Muller A 1990 *Phys. Rep.* **197** 167–262
[9] Kudo H, Maruyama M, Tanikawa M, Shinozuka T and Fujioka M 1998 *Phys. Rev.* C **57** 178–88
[10] Demekhina N A and Karapetyan G S 2008 *Phys. At. Nucl.* **71** 27–35
[11] Karapetyan G S, Balabekyan A R, Demekhina N A and Adam J 2009 *Phys. At. Nucl.* **72** 911–6
[12] Wagemans C, Schillebeeckx P and Deruytter A 1989 *Nucl. Phys.* A **502** 287–96
[13] Weber Th *et al* 1989 *Nucl. Phys.* A **502** 279–86
[14] Sida J L *et al* 1989 *Nucl. Phys.* A **502** 233–42
[15] Bockstiegel C, Steinhauser S, Schimdt K-H, Clerc H-G, Grewe A, Heinz A, de Jong M, Junghans A R, Muller J and Voss B 2008 *Nucl. Phys.* A **802** 12–25
[16] Hambsch F J, Oberstedt S, Vladuca G and Tudora A 2002 *Nucl. Phys.* A **709** 85–102
[17] Hambsch F J *et al* 2003 *Nucl. Phys.* A **726** 248–64
[18] Weigmann H, Knitter H H and Hambsch F J 1989 *Nucl. Phys.* A **502** 177–94
[19] Ohtsuki T *et al* 1989 *Phys. Rev.* C **40** 2144–53
[20] Duijvestijn M C *et al* 1999 *Phys. Rev.* C **59** 776–88
[21] Maslov V M 2003 *Nucl. Phys.* A **717** 3–20
[22] Itkis M G, Okolovich V N, Rusanov A Ya and Smirenkin G N 1985 *Z. Phys.* A **320** 433–41
[23] Pokrovsky I V *et al* 2000 *Phys. Rev.* C **62** 1–10
[24] Pereira J *et al* 2007 *Phys. Rev.* C **75** 044604
[25] Andrade II E, Freitas E, Tavares O A P, Duarte S B, Deppman A and Garcia F 2009 *AIP Conf. Proc.* **1139** 64–9
[26] Deppman A, Duarte S B, Silva G, Tavares O A P, Anefalos S, Arrudo Neto J D T and Rodrigues T E 2004 *J. Phys. G: Nucl. Part. Phys.* **30** 1991–2003
[27] Kodama T, Duarte S B, Chung K C and Nazareth R A M S 1982 *Phys. Rev. Lett.* **49** 536–9
[28] Goncalves M, dePina S, Lima D A, Milomen W, Medeiros E L and Duarte S B 1997 *Phys. Lett.* B **406** 1–6
[29] Deppman A, Tavares O A P, Duarte S B, de Oliveira E C, Arruda Neto J D T, de Pina S R, Likhachev V P, Rodriguez O, Mesa J and Goncalves M 2001 *Phys. Rev. Lett.* **87** 1–4
[30] de Pina S *et al* 1998 *Phys. Lett.* B **434** 1–6
[31] Deppman A, Tavares O A P, Duarte S B, de Oliveira E C, Arruda Neto J D T, de Pina S R, Likhachev V P, Rodriguez O, Mesa J and Goncalves M 2002 *Comput. Phys. Commun.* **145** 385–94
[32] Deppman A, Tavares O A P, Duarte S B, Arruda Neto J D T, Goncalves M, Likhachev V P and de Oliveira E C 2002 *Phys. Rev.* C **66** 067601
[33] Deppman A, Silva G, Anefalos S, Duarte S B, Garcia F, Hisamoto F H and Tavares O A P 2006 *Phys. Rev.* C **73** 1–5
[34] Anéfalos Pereira S, Deppman A, Silva G, Maiorino J R, dos Santos A, Duarte S B, Tavares O A P and Garcia F 2008 *Nucl. Sci. Eng.* **159** 102–5
[35] Anefalos S, Deppman A, Silva G, Maiorino J R, dos Santos A, Duarte S B, Tavares O A P and Garcia F 2005 *Braz. J. Phys.* **35** 912–4
[36] Anefalos S, Deppman A, Arruda Neto J D T, da Silva G, Maiorino J R, dos Santos A and Garcia F 2005 *AIP Conf. Proc.* **769** 1299–302
[37] Mongelli S T, Maiorino J R, Anefalos S, Deppman A and Carluccio T 2005 *Braz. J. Phys.* **35** 894–7
[38] Siegler P, Hambsch F-J, Oberstedt S and Theobald J P 1995 *Nucl. Phys.* A **594** 45–56
[39] Fernandez-Dominguez B *et al* 2005 *Nucl. Phys.* A **747** 227–67